

Laser Chemistry

First Highly Efficient and Photostable *E* and *C* Derivatives of 4,4-Difluoro-4-bora-3a,4a-diaza-*s*-indacene (BODIPY) as Dye Lasers in the Liquid Phase, Thin Films, and Solid-State Rods

Gonzalo Duran-Sampedro,^[a] Ixone Esnal,^[c] Antonia R. Agarrabeitia,^[a] Jorge Bañuelos Prieto,^[c] Luis Cerdán,^[b] Inmaculada García-Moreno,^{*[b]} Angel Costela,^[b] Iñigo Lopez-Arbeloa,^[c] and María J. Ortiz^{*[a]}

Abstract: A new library of *E*- and *C*-4,4-difluoro-4-bora-3a,4a-diaza-*s*-indacene (BODIPY) derivatives has been synthesized through a straightforward protocol from commercially available BODIPY complexes, and a systematic study of the photophysical properties and laser behavior related to the electronic properties of the B-substituent group (alkynyl, cyano, vinyl, aryl, and alkyl) has been carried out. The replacement of fluorine atoms by electron-withdrawing groups enhances the fluorescence response of the dye, whereas electron-donor groups diminish the fluorescence efficiency. As a consequence, these compounds exhibit enhanced laser action with respect to their parent dyes, both in liquid solution and in the solid phase, with lasing efficiencies under transversal pumping up to 73% in liquid solution and 53% in a solid

matrix. The new dyes also showed enhanced photostability. In a solid matrix, the derivative of commercial dye PM597 that incorporated cyano groups at the boron center exhibited a very high lasing stability, with the laser emission remaining at the initial level after 100 000 pump pulses in the same position of the sample at a 10 Hz repetition rate. Distributed feedback laser emission was demonstrated with organic films that incorporated parent dye PM597 and its cyano derivative. The films were deposited onto quartz substrates engraved with appropriate periodical structures. The *C* derivative exhibited a laser threshold lower than that of the parent dye as well as lasing intensities up to three orders of magnitude higher.

Introduction

Tunable lasers are an important tool in a wide variety of fields such as spectroscopy, photochemistry, material diagnosis, medicine, or integrated optical devices. Organic dye molecules offer clear advantages over other commercially available multi-wavelength laser sources such as low cost, ample spectral coverage over the visible region of the electromagnetic spectrum, and high conversion efficiency.^[1]

Among the numerous classes of highly fluorescent dyes used as the active media of tunable lasers, the family of difluoroboron dipyrromethene complexes, or BODIPYs, is one with the highest potential.^[2] Their development has acquired great importance in the last two decades owing to the excellent and easily modulated photophysical properties of these fluorophores.^[3] As a consequence, they are also intensively applied as fluorescent probes in biological systems, photosensitizers for photodynamic therapy, and as materials for incorporation into electroluminescent devices.^[2a,4]

The incorporation of appropriate functional groups into the chromophore could lead to new photophysical processes or large spectral shifts; therefore, depending on the desired application, one should carefully choose the kind of substituents and the position in which they will be incorporated into the BODIPY. A strategy that causes a substantial increase of the potential applications of the chromophore BODIPY is the substitution of fluorine atoms.^[3a-c] Thus, a wide variety of new BODIPYs have been synthesized by means of fluorine displacement by alkyl or aryl groups (*C*-BODIPYs), ethynyl groups (*E*-BODIPYs), and alkoxy or aryloxy groups (*O*-BODIPYs).^[5] The introduction of these functional groups leads to an increase in the Stokes shift as well as to the improved chemical and photochemical stability of these fluorophores, thereby opening the way to a new class of highly luminescent dyes.

[a] G. Duran-Sampedro, Prof. A. R. Agarrabeitia, Prof. M. J. Ortiz
Departamento de Química Orgánica I
Facultad de Ciencias Químicas, Universidad Complutense
28040 Madrid (Spain)
Fax: (+34) 913944103
E-mail: mjortiz@quim.ucm.es

[b] Dr. L. Cerdán, Prof. I. García-Moreno, Prof. A. Costela
Instituto de Química-Física "Rocasolano" (IQFR), CSIC
Serrano 119, 28006 Madrid (Spain)
Fax: (+34) 915642431
E-mail: i.garcia-moreno@iqfr.csic.es

[c] I. Esnal, Dr. J. Bañuelos Prieto, Prof. I. Lopez-Arbeloa
Departamento de Química Física, UPV-EHU
Apartado 644, 48080 Bilbao (Spain)

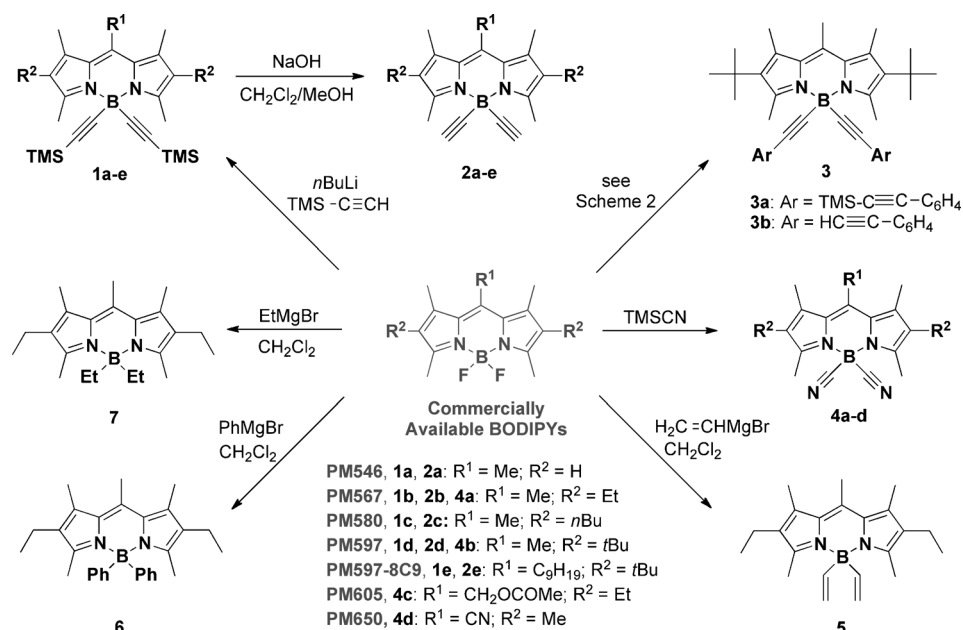
Supporting information for this article is available on the WWW under <http://dx.doi.org/10.1002/chem.201303579>.

Despite the considerable volume of work on the synthesis and applications of this type of fluorophores, there are few reports on their optical and lasing properties.^[5c,d] In this field, our research group has described the synthesis and characterization of the emission properties of a set of *O*-BODIPYs in which two carboxylate groups are connected to the boron center in place of the fluorine atoms. It was shown that these dyes are highly fluorescent and exhibit enhanced laser action with respect to their *F*-BODIPY analogues, both in liquid solution and the solid phase.^[5c]

Considering these results, in the present work we have synthesized a new library of *E*- and *C*-BODIPY derivatives (named 1–7 in Scheme 1) from the commercially available BODIPYs and we have carried out a systematic study of their photophysical properties and laser behavior related to the electronic properties of the B-substituent group (alkynyl, cyano, vinyl, aryl, and alkyl). As far as we know, there is only one precedent on lasing performance of *E*-BODIPYs by Ray et al. in which it is revealed that this substitution at the boron center does not significantly improve the laser efficiency but enhances the photostability owing to their lower reaction rates with ¹O₂ and lower ¹O₂ generation capacity.^[5d] However, the new BODIPY derivatives synthesized herein through a straightforward protocol exhibit lasing efficiencies up to four times higher than those recorded for the corresponding commercial dyes with high photostability in the liquid phase, the bulk solid state, and in thin films.

Results and Discussion

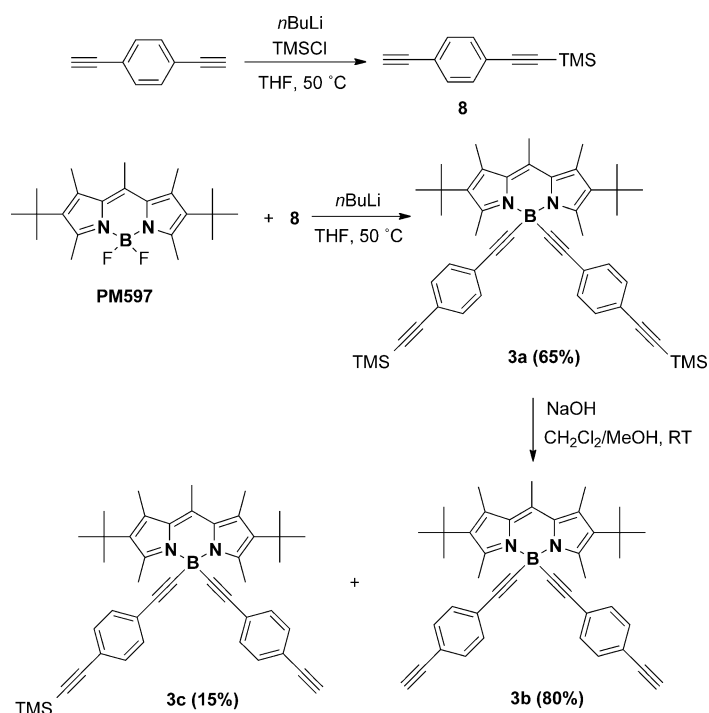
BODIPY dyes 1–7 were successfully obtained from commercially available dyes PM546, PM567, PM580, PM597, PM597-8C9, PM605, and PM650 with organolithium, Grignard reagents, or trimethylsilyl cyanide (TMSCN) as nucleophilic agents depending upon the desired change in the boron atom. BODIPY derivatives **1b**,^[6] **2b**,^[6] and **6**^[7] were synthesized by the methods previously described. Dyes **1a–e** were prepared in good yield by the introduction of two trimethylsilylacetylene units by using an excess amount of the corresponding organolithium derivative, generated in situ from trimethylsilylacetylene and *n*-butyllithium. No monosubstituted derivatives were formed under the reaction conditions. Removal of the trimethylsilyl groups using an excess amount of NaOH afforded **2a–e** as the major products. Only compound **2a** was obtained in addition to a small percentage of the monoprotected derivative.



Scheme 1. Molecular structures of commercial dyes and their analogues 1–7 synthesized in this work.

The reaction of PM597 with mono-TMS-protected 1,4-diethynylbenzene **8** gave *E*-BODIPY **3a** in good yield. The removal of the TMS protection yielded a mixture of dideprotected derivative **3b** (80%) and monodeprotected derivative **3c** (15%), which were separated by means of flash chromatography on silica (Scheme 2).

Replacement of the fluorine atoms by cyano groups (compounds **4a–d**) was carried out by the reaction of BODIPY with TMSCN in the presence of AlCl₃ as Lewis acid (compounds **4a**



Scheme 2. Synthesis of BODIPYs **3a–c**.

and **4c**) or in the absence of AlCl_3 (compounds **4b** and **4d**) in 82 to 85% yield, except for **4d**, which was obtained in 25% isolated yield.

Furthermore, the use of an excess amount of Grignard reagents (vinylmagnesium bromide or ethylmagnesium bromide) led to rapid substitution of the fluorine atoms and allowed the preparation of compounds **5** and **7**, respectively, in moderate yield.

Photophysical properties

The commercial *F*-BODIPYs that bear linear alkyl groups (PM546, PM567, and PM580) set themselves apart by their high fluorescence performance (approaching 100% in Figure 1 and Table S1 in the Supporting Information), although the fluorescence capacity of the BODIPYs depends on the functional-

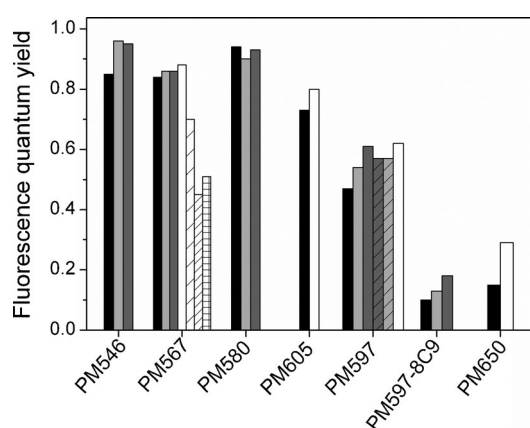


Figure 1. Fluorescence quantum yield in ethyl acetate of the commercial *F*-BODIPYs (black) and their corresponding *E*-BODIPYs bearing acetylene (**2a–e**, grey, striped if phenyl is also grafted, **3b**), acetylene TMS (**1a**, **1c–e**, light grey, striped upon addition of a phenyl, **3a**), and *C*-BODIPYs bearing a cyano (**4a–d**, white), vinyl (**5**, sparse stripe), ethyl (**7**, dense stripe), and phenyl group (**6**, grid).

ization of the core. Thus, the presence of methylenacetoxyl at the *meso* position (PM605) reduces the radiative deactivation probability owing to its electron-withdrawing character, whereas the *tert*-butyl groups (PM597 and PM597-8C9) enhance the nonradiative pathways owing to the geometrical distortion induced by the sterical hindrance to accommodate such bulky groups. The most noteworthy case is the appearance of a quenching intramolecular charge transfer (ICT) state by the grafting of the cyano at the central position (PM650).^[8]

The replacement of fluorine atoms in the above BODIPYs by acetylenes (**2a–e**) does not have a great impact on the photophysics of the chromophore (Figure 1). The fluorescence quantum yields of the resulting *E*-BODIPYs remain high (set of derivatives from PM546, PM567, and PM580), or at least similar to their corresponding counterpart (PM597). Moreover, the addition of trimethylsilyl (**1a**, **1c**, and **1d**), aryl (**3b**), or both (**3a**) onto the triple bond has a minor effect. These results are reasonable keeping in mind that the boron atom does not take part in the delocalized π system but acts as a bridge unit to

infer rigidity onto the whole structure. Indeed, opposite results (high bathochromic shifts and reduced fluorescence quantum yields) have been reported for acetylene groups directly attached to the core at the 2- and 6-positions.^[9]

Nevertheless, the electronic character of the group anchored to the boron atom plays a key role in the fluorescence performance of the resulting *E*- and *C*-BODIPY (Figure 1). Such an effect can be easily discussed by considering the set of derivatives from PM567. The acetylene group behaves like a weak electron acceptor (Hammett parameter $\sigma_p^+ = 0.18$). A further increase in such behavior through the presence of cyano groups ($\sigma_p^+ = 0.66$) results in an improvement in the fluorescence behavior (see compounds **4a–4d** in their respective series in Figure 1). Such an enhancement is especially noticeable in PM650 since the fluorescence quantum yield increases from 0.15 to 0.29. It is possible that the two cyano groups linked to the boron atom counteract the charge separation induced by the *meso*-cyano substitution to hamper the population of the ICT state. However, a withdrawing character that is too strong could damage the fluorescence performance, which is what happens in *O*-BODIPYs that bear nitro groups ($\sigma_p^+ = 0.74$) owing to the activation of ICT processes.^[5c]

By contrast, the presence of electron-donor groups, such as phenyl rings ($\sigma_p^+ = -0.18$), leads to a decrease in the fluorescence quantum yield and lifetime (Figure 1). Moreover, this compound (**6**) exhibits a high Stokes shift (1350 versus 550 cm^{-1} in PM567) as a result of a bathochromic shift of the fluorescence band (Figure 2). Such a trend suggests a high geometrical rearrangement upon excitation, which enables the energy relaxation and the consequent loss of fluorescence emission. In addition, the optimized excited-state geometry points to the high steric hindrance induced by the two rings attached to the boron (Figure S1 in the Supporting Information). As a result, the two phenyl groups are placed orthogonally and the chromophore is distorted (deviation from planarity up to 25°). This lack of planarity enhances the internal conversion and explains the recorded lower fluorescence performance for compound **6**.

Similar trends are observed with the unsaturation degree of the alkyl chains attached to the boron atom. A change from acetylene (compound **2b**) to vinyl (**5**) and to ethyl (**7**) implies a reversal of the electronic behavior from electron donor to acceptor ($\sigma_p^+ = 0.18$, -0.16 , and -0.30 , respectively). Accordingly, the fluorescence quantum yield and lifetime decrease in the same fashion (Figures 1 and 2). In fact, in the *C*-BODIPY that bears ethyl (compound **7**), the Stokes shift is quite high (1115 cm^{-1}) as a consequence of the shift of the fluorescence band towards lower energies. Again, the optimized excited-state geometry confirms the geometrical distortion (up to 23° ; Figure S2 in the Supporting Information) to be the main pathway for nonradiative deactivation.

The quantum mechanical calculations (Table 1) reproduce the experimental features well. Indeed, the absorption and fluorescence spectra signatures are satisfactorily predicted theoretically. Both compounds **6** and **7** stand out through an emission shifted to lower energies and a higher Stokes shift as result of an important change in the geometry upon excita-

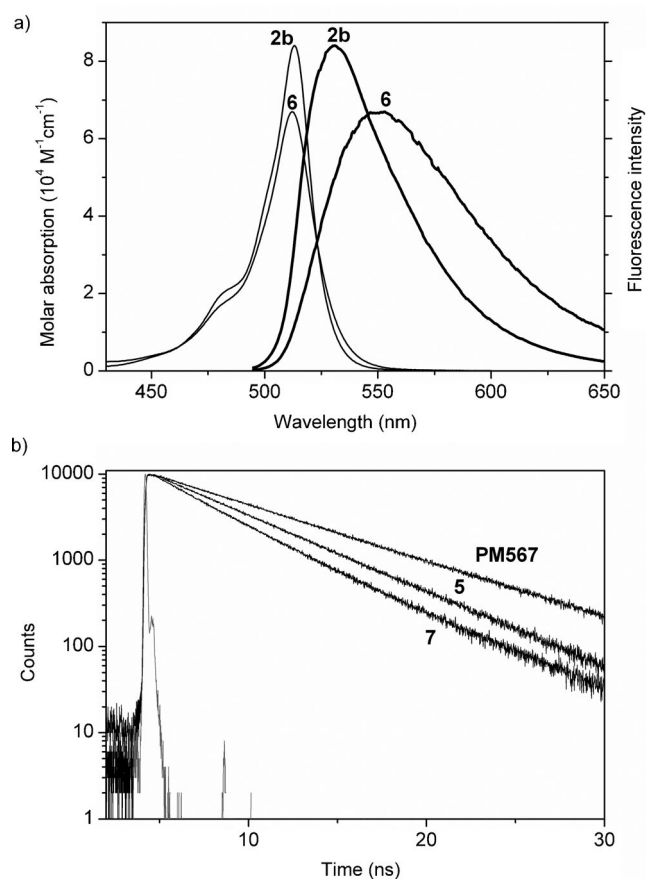


Figure 2. a) Absorption and normalized fluorescence (bold) spectra in ethyl acetate of PM567 derivatives bearing acetylene (**2b**) and phenyl (**6**) groups. b) Fluorescence decay curves of PM567 derivatives bearing vinyl (**5**) and ethyl (**7**) groups.

	ΔE_{ab} [eV]	ΔE_{fl} [eV]	$\Delta \nu_{st}$ [cm^{-1}]
PM567	2.91	2.87	380
2b	2.94	2.89	445
6	2.92	2.77	1210
5	2.95	2.88	580
7	2.99	2.83	1265
PM597	2.87	2.73	1170
PM597-8C9	2.84	2.62	1795

tion. Such theoretically suggested loss of planarity correlates well with the evolution of the nonradiative rate constant (Table S1 in the Supporting Information).

To address the opposite influence of the electron donor (harmful to the fluorescence capacity) and acceptor (slightly beneficial) groups, which are attached to boron in the *E*- and *C*-BODIPYs, we simulated the charge-density distribution in some selected compounds (Figure S3 in the Supporting Information). In a previous study on *O*-BODIPYs, we concluded that although the boron atom does not take part in the delocalized π system, its substitution determines the charge distribution

through the whole chromophore and hence the aromaticity of the π system (evaluated by the bond-length alternation (BLA) parameter,^[10] data included in Figure S3 in the Supporting Information).

The presence of acetylene groups leads to a higher positive charge in the boron atom and a slightly lower charge alternation through the core, with little influence on the aromaticity (similar BLA and fluorescence capacity to their corresponding reference *F*-BODIPYs). An increase in the electron-donor ability of the substituent (cyano groups) implies a strong rearrangement of the charge distribution, which results in a more aromatic chromophore, as reflected in the BLA parameter (i.e., 0.023 for compound **4a**), which is the lowest among all the BODIPYs reported herein. Accordingly, the derivatives with a cyano group at the boron atom (**4a–4d**) yield the highest fluorescence capacity. However, a progressive increase in the electron-donor ability of the substituent (from acetylene to ethyl) results in less aromatic dyes (BLA = 0.027, 0.029, and 0.031 for compounds **2b**, **5**, and **7**, respectively), which is in agreement with the registered lower fluorescence efficiencies. Especially remarkable is the asymmetric disposition of the phenyl rings in compound **6**. This should be a consequence of the steric hindrance between their *ortho*-hydrogen and the methyl groups in the 3- and 5-positions (Figure S1 in the Supporting Information). As a result, one of the rings acquires a high positive charge (Figure S3 in the Supporting Information) and leads to a less aromatic dye (BLA = 0.028), thereby reducing the fluorescence capacity.

Whereas the lengthening of the alkyl chain (from ethyl to butyl) at the 2- and 6-positions of PM567 to yield PM580 has a minor effect on the photophysical properties, important changes are noticed when the aliphatic chain is enlarged (from one methylene to nine) at the 8-position of PM597 to yield PM597-8C9 (Figure 1 and Table S1 in the Supporting Information). The photophysical properties of PM597 were controlled by the steric hindrance induced by the *tert*-butyl groups, which leads to a loss of planarity in the chromophore. As consequence, the nonradiative rate constant (from $0.28 \times 10^8 \text{ s}^{-1}$ in PM567 to $1.23 \times 10^8 \text{ s}^{-1}$ in PM597) and the Stokes shift (from 550 to 1330 cm^{-1} , respectively) increased significantly. These trends seem to be more evident upon grafting a linear chain at the 8-position, because the nonradiative rate (k_{nr}) enhances up to $7.9 \times 10^8 \text{ s}^{-1}$, thereby reducing the fluorescence quantum yield and lifetime (0.10 and 1.14 ns). In addition, the Stokes shift increases up to 2330 cm^{-1} as a result of a stronger bathochromic shift in the fluorescence band (placed at 595 nm, also theoretically predicted in Table 1).

The optimized geometries show that the linear chain in PM597-8C9 adopts a linear disposition, far away from the indacene core (Figure S1 in the Supporting Information). However, its presence seems to enhance the steric hindrance and a drastic geometrical rearrangement takes place after excitation. As a result, the chromophore geometry is highly distorted and a deviation of planarity up to 30° is predicted. Overall, such loss of planarity implies lower aromaticity, but surprisingly, the opposite happens in the compounds that bear 2,6-*tert*-butyl. In fact, the BLA parameters suggest that these compounds

Table 2. Lasing efficiencies of commercial BODIPY dyes and their C-BODIPY derivatives in different solvents at the dye concentrations that optimize their laser action of solutions in ethyl acetate (λ_{exc} : pumping wavelength).

Solvent	$\lambda_{\text{exc}} = 355 \text{ nm}$										$\lambda_{\text{exc}} = 532 \text{ nm}$																
	PM546	1a	2a	PM567	1b	2b	4a	5	6	7	PM580	1c	2c	PM597	1d	2d	3a	3b	4b	PM597-8C9	1e	2e	PM605	4c	PM650	4d	PM650-F-CN
EtOAc	23	58	52	48	67	60	68	54	60	30	57	65	63	53	70	63	73	68	73	55	62	59	55	68	35	45	36
Acetone	14	56	49	36	65	57	65	45	56	25	57	63	62	50	67	62	71	65	70	52	59	56	57	69	31	40	30
MeOH				34	58	54	61		52		51	61	57	54	63	59	69	63	68	47	59	54	55	66	12	30	22
EtOH	18	58	50	36	62	56	63	44	54	27				51	65	61	69	60	67				56	67			
F ₃ -EtOH														56	63	57	70	62	65				51	61	27	38	28
CH ₂ Cl ₂											50	61	59							50	60	56					
THF											59	66	64														

(PM597 and PM597-8C9) become more aromatic as the excited-state distortion increases (BLA of 0.022 and 0.019, respectively). These evolutions have been previously reported and explained in terms of the “loose-bolt” or Brunings–Corwin effect, in which the lower planarity by constrained geometries implies a lower resonance energy, thereby placing the excited and ground states energetically closer.^[11] Therefore, the strong bending of the chromophore in the excited state should be the reason for the important shift of the emission band towards higher energies and, at the same time, the reason for the reduction of the fluorescence efficiency in those compounds that bear *tert*-butyl groups at the 2- and 6-positions (PM597 and mainly PM597-8C9). In these dyes, further replacement of the fluorine atoms by acetylene (**1 e**, **2 e**) slightly ameliorates the fluorescence capacity, in line with the previously discussed *E*- and C-BODIPYs.

Lasing properties

Liquid phase

According to their absorption properties, the lasing properties of PM546 and its derivatives **1 a** and **2 a** were studied under pumping at 355 nm, whereas all the other dyes studied here were pumped at 532 nm. The dye concentrations in the lasing studies are in the millimolar range, as required by our experimental conditions of transversal excitation and strong focusing of the incoming pump radiation. In this way, the pump radiation is totally absorbed within the first millimeter of the solution to obtain an emitted laser beam with a near-circular cross-section.

To optimize the laser action, for the different dyes we first analyzed the dependence of their laser emission on dye concentration in ethyl acetate. The results obtained by varying the dye concentrations over the range 0.3 to 10 mM, depending on the dye, while keeping all the other experimental parameters constant, are collected in Table S2 in the Supporting Information. In all cases the dyes followed the typical behavior, with the lasing efficiency (defined as the ratio between the energy of the dye laser output and the pump energy incident on the sample surface) first increasing with dye concentration until a maximum value is reached. Increasing the dye concentration beyond this point results in a decrease in the lasing efficiency that can be related to reabsorption/reemission processes,

which become increasingly important as the dye concentration rises. The optimum value of the dye concentration thus determined was then used to prepare dye solutions in a number of polar protic and polar aprotic solvents to analyze the effect of the nature of the solvent on the laser properties of the different derivatives. The results obtained are collected in Table 2.

The observed lasing efficiencies within the different families of *E*- and C-BODIPYs correlate well with their photophysical properties, determined in more diluted solutions (Tables S1 and S2 in the Supporting Information): higher lasing efficiency corresponds in general to a lower nonradiative rate constant. The few exceptions to this general rule (i.e., in the PM580 family) can be understood in terms of the effect of the much higher dye concentration in the solutions utilized in the laser experiments.

The lasing properties of the new dyes follow a dependence on the solvent character similar to that exhibited by the commercial ones, with the lasing efficiencies being higher in polar aprotic solvents than in polar protic ones. It can be seen in Table 2 that, with the exception of dye **7**, in all cases the lasing efficiency of the derivatives is higher than that of the commercial parent dye. The highest lasing efficiencies were obtained with the derivatives that incorporate cyano groups (compounds **4 a–d**), which is in agreement with their photophysical behavior discussed above. The improvement in their fluorescence capacity was owing to the action of the cyano group counteracting the charge separation as a result of the increased electron-donor ability of the cyano substituent. The effect of the unsaturation degree of the alkyl chains attached to the boron atom, discussed in detail above, is also clearly indicated by the lasing data. Thus, the change from acetylene (compound **2 b**) to vinyl (**5**) and to ethyl (**7**), which produces a reversal of the electronic behavior from electron donor to acceptor as well as an increased geometrical distortion in the excited-state geometry of those compounds, takes place in accord with a decrease in the lasing efficiency following the sequence $\text{Eff}(\mathbf{2b}) > \text{Eff}(\mathbf{5}) > \text{Eff}(\mathbf{7})$ (Table 2).

An important parameter for any practical application of dye lasers is their lasing photostability under repeated pumping. Table 3 collects the data on the decrease in the laser-induced fluorescence intensity under transversal excitation of a capillary that contains dye solutions in ethyl acetate (see the Experi-

Table 3. Intensity of the laser-induced fluorescence emission (I) after 100 000 pump pulses for dyes in ethyl acetate solution.

	$\lambda_{\text{exc}} = 355 \text{ nm}$										$\lambda_{\text{exc}} = 532 \text{ nm}$														
	PM546	1a	2a	PM567	1b	2b	4a	6	7	PM580	1c	2c	PM597	1d	2d	3a	3b	4b	PM597-8C9	1e	2e	PM605	4c	PM650	4d
I [%] ^[a]	60	92	76	17	55	70	100	100	50	48	84	70	85	100	94	65	72	100	30 ^[b]	100	100	20 ^[c]	100	80	75

[a] I [%] = 100 (I/I_0), with I_0 being the initial intensity. [b] After 60 000 pump pulses. [c] After 40 000 pump pulses.

mental Section) after a given number (n) of pump pulses for both the commercial dyes and their derivatives synthesized in the present work. Dye PM546 and its derivatives **1a** and **2a** were pumped at 355 nm and at 5 Hz repetition rate. All the other dyes were pumped at 532 nm and at a 10 Hz repetition rate. The pump energy was 5 mJ in all cases. Dyes **4a–c**, which exhibited the highest lasing efficiencies and the best photophysical behavior, also were the most photostable, with their laser-induced fluorescence emission remaining at the initial level after 100 000 pump pulses. This stability is significantly higher than that of the corresponding commercial dyes (PM567, PM597, and PM605). Compound **4d**, which is the derivative of the *meso*-cyano-substituted dye PM650, exhibits lower photostability than **4a–c**, thereby reflecting the presence of the ICT state in PM650 with its harmful effects on laser performance and stability.^[8]

Bulk solid state

The excellent laser performance exhibited by the new dyes in liquid solution led us to explore their behavior as photonic materials, either in bulk as solid-state dye lasers (SSDLs) or incorporated into thin-film structures. First, we analyzed the laser behavior of the dyes incorporated into bulk solid samples cast in a cylindrical shape, thereby forming rods 10 mm in diameter and 10 mm in length (for more details, see the Supporting Information). The dyes chosen to perform this study were **4a–4c** because of their excellent lasing properties in liquid solution, and their behavior as SSDLs was compared with the corresponding parent dyes PM567, PM597, and PM605, respectively. As matrix material we chose poly(methylmethacrylate) (PMMA) because it mimics ethyl acetate, the solvent in which those dyes produced the highest lasing efficiencies (Table 2). In addition, PMMA has very high transparency, high laser damage threshold, very good chemical compatibility with the chosen dyes, and, most importantly from a practical point of view, the final production costs would be low owing to its cheapness. The dye concentration in the matrix was that which optimized the lasing efficiency in ethyl acetate (Table S2 in the Supporting Information).

Table 4 contains the lasing performance of the selected dyes. The lasing efficiencies of the C-BODIPYs enhanced significantly those obtained with the corresponding commercial parent dyes, and correlate with those obtained in liquid solution, with the efficiency of dye **4b** being the highest. These efficiencies are lower than those obtained in liquid solution, probably owing to the fact that the finishing of the surface of the solid samples relevant to the laser operation was not laser-

Table 4. Lasing properties of dyes incorporated into solid PMMA matrices.^[a]

Dye	Eff [%]	λ_1 [nm]	I_n [%]	n
PM567	34	566	30	100 000
4a	49	568	96	100 000
PM597	36	585	85	100 000
4b	53	588	100	100 000
PM605	37	595	0	65 000
4c	51	597	80	100 000

[a] Eff: lasing efficiency; λ_1 : peak laser emission wavelength; I_n [%]: intensity of the laser output after n pump pulses in the same position of the sample; I_n [%] = 100 (I_n/I_0), with I_0 being the initial intensity.

grade, so that higher efficiencies are to be expected with laser-grade surfaces.

To assess the photostability of the new materials, we followed the evolution of their laser emission under repeated pumping in the same position of the sample at a repetition rate of 10 Hz. All three derivatives demonstrated a much higher photostability than the parent dyes, with dye **4b**, which has a laser emission that remains at the initial level after 100 000 pump pulses in the same position of the sample, exhibiting the best behavior once again. These results show that the newly developed C-BODIPYs are excellent candidates to achieve SSDLs with greatly improved performance.

Thin films

As a proof of concept, we also assessed the laser properties of the new BODIPYs operated as dye-doped polymer thin-film lasers, since over the last few years there has been a growing interest in the development of these types of devices because of their potential applications as coherent light sources suitable for integration in spectroscopic and sensing devices.^[12]

Given the outstanding laser properties shown by derivative **4b** both in liquid and the solid state, we decided to choose this dye and its parent dye PM597 as reference to develop the thin-film laser. The host matrix was PMMA. Thin films approximately 800–850 nm thick were prepared from solution by solving adequate amounts of dye and PMMA in chloroform, and the resulting solutions were spin-coated onto quartz substrates. The complete details on the sample preparation and evaluation can be found in the Supporting Information.

To obtain sufficient pump absorption and gain in the thin films, dye concentrations were selected to render an absorbance of 0.08 at the pump wavelength (532 nm). This means concentrations of 19 and 23 mM for PM597 and derivative **4b**,

respectively. Such high concentrations are prone to give rise to self-quenching^[13] (mirrored as band displacements and reduction in fluorescence quantum yield and extinction coefficients) and aggregate formation^[11] (appearance of new absorption bands). To assess the extent of both phenomena, the absorption and emission spectra of both dyes were collected (Figure 3). Even at these high dye concentrations, the absorp-

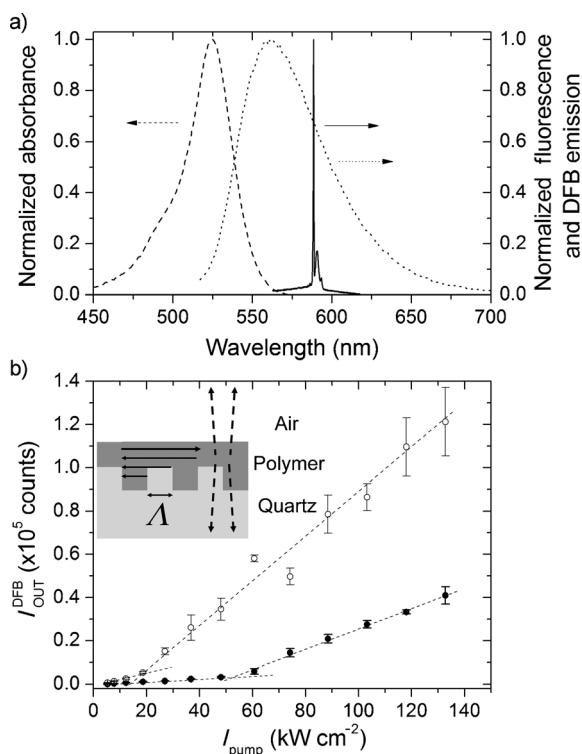


Figure 3. a) Absorption (dashed line), fluorescence ($\lambda_{\text{exc}} = 500$ nm, dotted line), and laser spectra (solid line) of derivative **4b** (23 mM) doped in PMMA. b) DFB output intensity as a function of pump intensity from thin films of commercial PM597 19 mM (filled circles) and derivative **4b** (23 mM; hollow circles) doped in PMMA. Inset: sketch of DFB laser. The arrows represent in-plane feedback owing to second-order diffraction (solid arrows) and out-coupled laser emission owing to first-order diffraction (dashed arrow).

tion and fluorescence spectra are redshifted by 2.5 and 0.5 nm, respectively, with respect to the ones registered with the dilute solutions, whereas the band shapes are unchanged (i.e., there are no new spectral features; compare Figures 2a and 3a). Nevertheless, the extinction coefficients of PM597 and derivative **4b** are reduced from 7.7 and $6.7 \times 10^4 \text{ M}^{-1} \text{ cm}^{-1}$ (2×10^{-6} M in EtOAc) to approximately 6.2 and $5.2 \times 10^4 \text{ M}^{-1} \text{ cm}^{-1}$ (≈ 20 mM in PMMA), respectively. The fluorescence quantum yield was not measured for the thin films, so it cannot be compared with the one in dilute solutions, but it will be arguably lower in the thin films. The previous facts indicate that dyes PM597 and derivative **4b** will suffer from a certain amount of self-quenching (but no aggregation) in the thin films, but we will see that it is not enough to prevent laser action from taking place.

To obtain resonant oscillation within the thin film, we made use of distributed feedback (DFB) owing to Bragg scattering in periodic structures (Figure 3b, inset).^[14] The emission wave-

length (λ_{DFB}) in DFB lasers is given by the Bragg condition $m \cdot \lambda_{\text{DFB}} \approx 2n_{\text{eff}} \Lambda$, in which m is the diffraction order in which the device operates, n_{eff} is the effective refractive index experienced by the propagating mode, and Λ is the period of the refractive index modulation (Figure 3b, inset). By working with the second-order $m = 2$, $\lambda_{\text{DFB}} \approx n_{\text{eff}} \Lambda$, the second-order diffraction provides in-plane feedback, and the laser light is diffracted out of the surface of the film perpendicular to the plane of the waveguide through first-order diffraction (Figure 3b, inset). The fundamental transverse electric (TE_0) propagating mode in waveguides approximately 800–850 nm thick with a refractive index of 1.4900 (PMMA), deposited onto a quartz substrate ($n = 1.456$), experiences an effective refractive index $n_{\text{eff}} = 1.472$.^[15] By taking into account that the resonant wavelength must be in the emission window of the selected dyes ($\lambda_{\text{DFB}} \approx 590$ nm), a substrate with modulation period $\Lambda = 400$ nm was used. For the present experiments, the quartz substrate was scribed by e-beam lithography^[16] with a squared grating (Figure 3b, inset) of period $\Lambda = 400$ nm, a duty cycle of 50%, and a depth of 100 nm. These waveguides might sustain a second propagating mode, the fundamental transverse magnetic (TM_0) mode, which does not participate in the laser process. We have excited the samples with the pump polarization parallel to the grating grooves so that the transition dipole moment of the emitting molecules and the grating wave vector (which is perpendicular to the grooves and parallel to the structure) fully overlap. This way the laser threshold of the TE_0 mode is maximally reduced.^[17]

By pumping the devices well above the threshold ($I_{\text{pump}} = 130 \text{ kW cm}^{-2}$), DFB laser emission with a linewidth of approximately 0.2 nm centered at 587.6 (PM597) and 588.5 nm (derivative **4b**) was obtained (Figure 3a), which is in agreement with the Bragg resonant wavelength expected for the chosen corrugated substrate and film thickness. The difference in the emission wavelengths is consistent with the slight changes in the sample thicknesses ($\approx \pm 50$ nm) owing to the deposition process, which modifies the effective refractive index n_{eff} and, in turn, the resonant wavelength.

Figure 3b shows the dependence of the DFB laser intensity on the pump intensity (light/light curve) for the samples doped with PM597 (filled circles) and derivative **4b** (hollow circles). From this plot one can determine the laser thresholds, which are the points in which there is a change in slope in the light/light curve. From the data in Figure 3b it can be seen that derivative **4b** not only has a lower DFB laser threshold than the parent dye (20 versus 55 kW cm^{-2}) but presents a threefold enhancement in the output intensity when pumped well above threshold ($I_{\text{pump}} = 130 \text{ kW cm}^{-2}$), which is in agreement with the results obtained in bulk and liquid media.

Conclusion

We have successfully designed and synthesized new *E*- and *C*-BODIPYs through a straightforward protocol from the commercially available BODIPYs. The experimental trends of the fluorescence efficiencies with the electron-donor/-acceptor properties of the substituents (Hammett parameter) at the boron

atom are properly rationalized by means of theoretical calculations in terms of the charge distribution and aromaticity (BLA) and excited-state geometry. Accordingly, the replacement of fluorine atoms by electron-acceptor moieties improves the fluorescence performance of commercial BODIPYs, whereas the electron-donor ones are harmful and lead to distorted geometries that enhance the nonradiative relaxation pathways.

The newly synthesized *E*- and *C*-BODIPYs exhibit enhanced laser action with respect to their parent dyes, both in liquid and in the solid phase, with the lasing properties correlating well with their photophysical behavior. The highest lasing efficiencies, up to 73% in the liquid phase and up to 53% in solid matrix under demanding transversal pumping conditions, were obtained with the derivatives that incorporated cyano groups at the boron center. These same derivatives also proved to be the most photostable, with stabilities significantly higher than that of the corresponding commercial dyes. Particularly relevant was the behavior of dye **4b** in solid matrix, which exhibited a very high lasing stability, with the laser emission remaining at the initial level after 100 000 pump pulses in the same position of the sample at 10 Hz repetition rate.

DFB laser emission was demonstrated with organic films that incorporated parent dye PM597 and its derivative **4b**, deposited onto quartz substrates engraved with appropriate periodical structures. Derivative **4b** exhibited a laser threshold lower than that of the parent dye as well as lasing intensities up to three orders of magnitude higher.

These results show that the newly developed *E*- and *C*-BODIPYs are excellent candidates to achieve SSDLs with much improved performance.

Experimental Section

BODIPY dyes PM546, PM567, PM580, PM597, P597-8C9, PM605, and PM650 were purchased from Exciton and used as received (purity >99%). Experimental procedures, characterization, and NMR spectra of the new dyes as well as quantum mechanical simulations, preparation of laser samples, and methods followed to analyze the photophysical and laser properties in the liquid and solid phase are described in detail in the Supporting Information.

Acknowledgements

This work was supported by the Ministerio de Economía y Competitividad (projects MAT2010-20646-C04-01, MAT2010-20646-C04-02, and MAT2010-20646-C04-04) and Gobierno Vasco (project IT339-10), which is also thanked by I.E. for a contract (SPE12UN140 and SPE13UN). G.D.-S thanks the MICINN for a predoctoral scholarship (FPI, cofinanced by Fondo Social Europeo).

Keywords: donor–acceptor systems · dyes/pigments · laser chemistry · photophysics · polymers

- [1] a) *Dye Laser Principles* (Eds.: F. J. Duarte, L. W. Hillman), Academic Press, New York, **1990**; b) *Tunable Lasers Handbook* (Ed.: F. J. Duarte), Academic Press, New York, **1995**; c) *Tunable Laser Applications*, 2nd ed. (Ed.: F. J.

- Duarte), CRC, Boca Raton, **2009**; d) I. D. W. Samuel, G. A. Turnbull, *Chem. Rev.* **2007**, *107*, 1272–1295.
- [2] a) M. Benstead, G. H. Mehl, R. W. Boyle, *Tetrahedron* **2011**, *67*, 3573–3601; b) Y. Xiao, D. Zhang, X. Qian, A. Costela, I. García-Moreno, V. Martín, M. E. Pérez-Ojeda, J. Bañuelos, L. Gartzia, I. López Arbeloa, *Chem. Commun.* **2011**, *47*, 11513–11515; c) J. Bañuelos, V. Martín, C. F. A. Gómez-Duran, I. J. Arroyo Cordoba, E. Peña-Cabrera, I. García-Moreno, A. Costela, M. E. Pérez-Ojeda, T. Arbeloa, I. López Arbeloa, *Chem. Eur. J.* **2011**, *17*, 7261–7270; d) G. Duran-Sampedro, A. R. Agarrabeitia, I. García-Moreno, A. Costela, J. Bañuelos, T. Arbeloa, I. López Arbeloa, J. L. Chiara, M. J. Ortiz, *Eur. J. Org. Chem.* **2012**, 6335–6358.
- [3] a) T. Bura, P. Retailleau, R. Ziessel, *Angew. Chem.* **2010**, *122*, 6809–6813; *Angew. Chem. Int. Ed.* **2010**, *49*, 6659–6663; b) C. Thivierge, A. Loudet, K. Burgess, *Macromolecules* **2011**, *44*, 4012–4015; c) C. A. Osorio-Martínez, A. Urías-Benavides, C. F. A. Gómez-Durán, J. Bañuelos, I. Esnal, I. López Arbeloa, E. Peña-Cabrera, *J. Org. Chem.* **2012**, *77*, 5434–5438; d) Y. Yang, Q. Guo, H. Chen, Z. Zhou, Z. Guo, Z. Shen, *Chem. Commun.* **2013**, *49*, 3940–3942.
- [4] a) A. Loudet, K. Burgess, *Chem. Rev.* **2007**, *107*, 4891–4932; b) R. Ziessel, G. Ulrich, A. Harriman, *New J. Chem.* **2007**, *31*, 496–501; c) G. Ulrich, R. Ziessel, A. Harriman, *Angew. Chem.* **2008**, *120*, 1202–1219; *Angew. Chem. Int. Ed.* **2008**, *47*, 1184–1201; d) F. L. Arbeloa, J. Bañuelos, V. Martínez, T. Arbeloa, I. L. Arbeloa, *Trends Phys. Chem.* **2008**, *13*, 101–122; e) A. C. Benniston, G. Copley, *Phys. Chem. Chem. Phys.* **2009**, *11*, 4124–4131; f) N. Boens, V. Leen, W. Dehaen, *Chem. Soc. Rev.* **2012**, *41*, 1130–1172; g) S. G. Awuah, Y. You, *RSC Adv.* **2012**, *2*, 11169–11183; h) A. Kamkaew, S. H. Lim, H. B. Lee, L. V. Kiew, L. Y. Chung, K. Burgess, *Chem. Soc. Rev.* **2013**, *42*, 77–88.
- [5] For example, see: a) S.-L. Niu, C. Massif, G. Ulrich, P.-Y. Renard, A. Romieu, R. Ziessel, *Chem. Eur. J.* **2012**, *18*, 7229–7242; b) A. Kaloudi-Chantzea, N. Karakostas, F. Pittler, C. P. Raptopoulou, N. Glezos, G. Pistolis, *Chem. Commun.* **2012**, *48*, 12213–12215; c) G. Durán-Sampedro, A. R. Agarrabeitia, L. Cerdán, M. E. Pérez-Ojeda, A. Costela, I. García-Moreno, I. Esnal, J. Bañuelos, I. López Arbeloa, M. J. Ortiz, *Adv. Funct. Mater.* **2013**, *23*, 4195–4205 and references cited therein; d) K. K. Jagtap, N. Shivran, S. Mula, D. B. Naik, S. K. Sarkar, T. Mukherjee, D. K. Maity, A. K. Ray, *Chem. Eur. J.* **2013**, *19*, 702–708; e) R. Ziessel, G. Ulrich, A. Haefele, A. Harriman, *J. Am. Chem. Soc.* **2013**, *135*, 11330–11344.
- [6] C. Goze, G. Ulrich, R. Ziessel, *Org. Lett.* **2006**, *8*, 4445–4448.
- [7] L. Yang, R. Simionescu, A. Lough, H. Yan, *Dyes Pigm.* **2011**, *91*, 264–267.
- [8] F. Lopez Arbeloa, J. Bañuelos, V. Martínez, T. Arbeloa, I. Lopez Arbeloa, *Int. Rev. Phys. Chem.* **2005**, *24*, 339–374.
- [9] I. García-Moreno, L. Wang, A. Costela, J. Bañuelos, I. Lopez Arbeloa, Y. Xiao, *ChemPhysChem* **2012**, *13*, 3923–3931.
- [10] G. Bourhill, J. L. Bredas, L. T. Cheng, S. R. Marder, F. Meyers, J. W. Perry, B. G. Tiemann, *J. Am. Chem. Soc.* **1994**, *116*, 2619–2620.
- [11] a) L. J. E. Hofer, R. J. Grabenstetter, E. O. Wiig, *J. Am. Chem. Soc.* **1950**, *72*, 203–209; b) M. Dekhtyar, W. Rettig, M. Szczepan, *Phys. Chem. Chem. Phys.* **2000**, *2*, 1129–1136; c) J. Bañuelos Prieto, F. López Arbeloa, V. Martínez, T. Arbeloa, I. López Arbeloa, *J. Phys. Chem. A* **2004**, *108*, 5503–5508; d) A. Costela, I. García-Moreno, M. Pintado-Sierra, F. Amat-Guerri, R. Sastre, M. Liras, F. López Arbeloa, J. Bañuelos Prieto, I. López Arbeloa, *J. Phys. Chem. A* **2009**, *113*, 8118–8124.
- [12] C. Grivas, M. Pollnau, *Laser Photonics Rev.* **2012**, *6*, 419–462.
- [13] F. López Arbeloa, T. López Arbeloa, I. López Arbeloa, I. García-Moreno, A. Costela, R. Sastre, F. Amat-Guerri, *Chem. Phys.* **1998**, *236*, 331–341.
- [14] T. T. Vu, M. Dvorko, E. Y. Schmidt, J.-F. Audibert, P. Retailleau, B. A. Trofimov, R. B. Pansu, G. Clavier, R. Méallet-Renault, *J. Phys. Chem. C* **2013**, *117*, 5373–5385.
- [15] Online 1D multilayer slab waveguide mode solver by Dr. Manfred Hammer, <http://wwwhome.math.utwente.nl/hammer/oms.html>.
- [16] G. A. Turnbull, A. Carleton, G. F. Barlow, A. Tahraoui, T. F. Krauss, K. A. Shore, I. D. W. Samuel, *J. Appl. Phys.* **2005**, *98*, 023105.
- [17] D. Wright, E. Brasselet, J. Zyss, G. Langer, W. Kern, *J. Opt. Soc. Am. B* **2004**, *21*, 944–950.

Received: September 10, 2013

Revised: November 18, 2013

Published online on January 22, 2014